Observation of Large Quadrupolar Effects in a Slow Photoelectron Imaging Experiment

F. Lépine, S. Zamith, A. de Snaijer, Ch. Bordas,* and M. J. J. Vrakking

FOM Institute for Atomic and Molecular Physics (AMOLF), Kruislaan 407, 1098 SJ Amsterdam, The Netherlands

(Received 27 July 2004; published 30 November 2004)

We have studied nondipolar effects in resonance-enhanced multiphoton ionization of Xe and have observed an azimuthal dependence of the photoelectron angular distribution on a quadrupole resonance, as well as a very large asymmetry with respect to the direction of the laser propagation close to the resonance, which is understood in terms of interference between dipole- and quadrupole-allowed ionization channels. The observed asymmetry in the photoelectron angular distribution provides insight into the ejection of slow photoelectrons near an ionization threshold.

DOI: 10.1103/PhysRevLett.93.233003 PACS numbers: 32.80.Rm, 07.81.+a, 32.60.+i, 32.80.Fb

In recent years there has been a renewed interest in the occurrence of nondipolar effects in atomic and molecular photoionization [1,2]. While it has been understood for many years that nondipolar effects can become important at photon energies beyond 1 keV, it was only recently realized that they can play a role at significantly lower energies as well, if differential rather than integral photoionization cross sections are considered. In the dipole approximation, spatial variations of the electric component of the electromagnetic field are assumed to occur on length scales that are large compared to the spatial extension of the atom. If the electric field of a laser propagating along the z axis is expanded as $\vec{E}(t)\exp(i\vec{k}\cdot\vec{z}) \approx \vec{E}(t)(1 + i\vec{k}\cdot\vec{z} + \cdots)$, where $\vec{k}$ is the wave vector of the light and z the coordinate of the electron along the laser propagation axis, the dipole approximation amounts to maintaining only the leading term in the expansion of $\exp(i\vec{k}\cdot\vec{z})$. As a consequence the interaction does not depend on the spatial coordinates of the atom or the direction of the light propagation, but only on the light polarization. In other words, the atom experiences a spatially homogeneous electric field and, due to symmetry, the angular distribution of the emitted photoelectrons depends only on the polar angle θ between the electron momentum and the light polarization. The dipole approximation is limited to situations where $kz \ll 1$ and thus $z \ll \lambda$. A breakdown in the dipole approximation may thus be anticipated when the spatial extension of the wave function becomes comparable to the wavelength of the light, as may occur when the wavelength of the radiation is small or in the case of "large" atoms (Rydberg states). When the dipole approximation breaks down, the cylindrical symmetry of the photoelectron angular distribution (PAD) around the laser polarization axis is lost, and the photoelectron angular distribution may depend on the direction of propagation of the light and the azimuthal angle ϕ.

The leading nondipolar term in photoionization arises due to electric quadrupole ($E2$) interactions. Using synchrotron radiation, anisotropy of photoelectron angular distributions with respect to the direction of light propagation has been observed in one-photon ionization at high photon energies [3,4], while recently significant quadrupole effects were observed in Xe at energies as low as 24 eV, exploiting the existence of a Cooper minimum in the $5s \rightarrow \varepsilon p$ dipolar transition amplitude [1]. Alternatively, exploiting the sensitivity of nondipolar effects to the spatial extension of the atom, forward/backward asymmetries in PADs for the ionization of Rydberg atoms have been observed with UV light, at photoelectron kinetic energies of just a few eV [5]. In most of these previous experiments the nondipolar effects were relatively small, the forward/backward asymmetries typically amounting to a few percent.

The possible importance of nondipolar terms in multiphoton ionization was pointed out early on by Lambropoulos *et al.* [6]. They discussed the feasibility of an experiment where a laser is tuned near a quadrupole resonance, so that (1 + 1) resonance-enhanced multiphoton ionization (REMPI) via this resonance becomes competitive with nonresonant two-photon ionization according to dipolar selection rules. Indeed, several groups have since published experimental results where multiphoton ionization was studied with a laser tuned to a quadrupole resonance [7–9], and where the on-resonance θ dependence was measured. Though also predicted by Lambropoulos *et al.* in Ref. [6], there have thus far been no experiments where the azimuthal (ϕ) dependence of the PAD occurring in REMPI via a quadrupole resonance has been reported.

In this Letter, we present observations of very large quadrupolar effects in two-photon ionization of Xe. Using two-dimensional photoelectron imaging, the azimuthal dependence of the PAD is investigated when the laser wavelength is tuned around the $6s[3/2]_{J=2} \rightarrow 5d[5/2]_{J=3}$ quadrupole resonance. Observations are made where the importance of the two-photon matrix elements involving the (near)-resonant quadrupolar excitation is enhanced and becomes comparable to the nonresonant dipolar two-photon matrix elements. In the experiment, the final energy after two-photon excitation falls between the saddle point in the Coulomb + dc field

potential and the field-free atomic ionization limit. Therefore the final kinetic energy of the photoelectrons is very low (typically 10 meV), and the observed quadrupolar asymmetries provide insight into the escape of the electrons over the saddle point.

In the experiment, photoelectrons resulting from the photoionization of metastable Xe atoms were detected using a velocity map imaging setup [10] extended with an electrostatic magnification lens in the drift region [11]. An 825 V/cm dc electric field accelerates the photoelectrons towards a position-sensitive detector consisting of two microchannel plates followed by a phosphor screen and a CCD camera that records the positions of electron impact and thus measures the PAD. The Xe atoms were prepared in the $6s[3/2]_{J=2}$ metastable state using an electron impact source. They were ionized by a tunable dye laser (Quanta-Ray PDL-3, bandwidth 0.1 cm^{-1}) that was tuned around the dipole-forbidden quadrupole-allowed $6s[3/2]_{J=2} \rightarrow 5d[5/2]_{J=3}$ resonance ($\Delta E = 15\,362.673\ cm^{-1}$). Experiments were performed with the laser propagation parallel to the detector plane and the laser polarization either parallel or perpendicular to this plane. The former geometry allows an observation of the polar (θ) dependence of the PAD, whereas the latter allows a direct observation of the azimuthal (ϕ) dependence of the PAD. Images were recorded at different wavelengths around the quadrupole resonance in a range of several 10 cm^{-1}.

Figure 1 represents a measurement at the $6s[3/2]_{J=2} \rightarrow 5d[5/2]_{J=3}$ quadrupole resonance with the laser polarization perpendicular to the detection plane. The image contains several features that are understood on the basis of our earlier work [12–14], namely, (i) an inner and outer contribution extending to radii R_I and R_{II}, and (ii) a number of interference rings that are especially clear in the inner contribution. The two contributions extending to R_I and R_{II} correspond to electrons moving along quasiparabolic "direct" trajectories and nonparabolic "indirect" trajectories (that are strongly influenced by Coulomb interactions with the Xe^+ core), respectively [see Fig. 3(a)] [12]. The interference structure that can be seen in the direct contribution (and at other wavelengths in the indirect contribution) is due to the fact that the electron can reach a particular point of the detector via several trajectories [see Fig. 3(a)] [14].

The PAD in Fig. 1 shows a breakdown of the cylindrical symmetry around the laser polarization axis. The photoelectrons are preferentially emitted along the direction of the light propagation, as shown in the lower panel of Fig. 1 for the direct contribution. Though azimuthally dependent, the PAD in Fig. 1 is symmetric with respect to the propagation direction of the laser. This changes in Figs. 2(a) and 2(b), where the frequency of the laser is tuned above or below the resonance. In this situation the PAD is azimuthally dependent and, moreover, displays a large forward/backward asymmetry. Photoelectrons are mainly emitted backward with respect to the light propagation when $\omega_{laser} > \omega_{res}$ [Fig. 2(a)], whereas the asymmetry is reversed for $\omega_{laser} < \omega_{res}$ [Fig. 2(b)]. Far away from the quadrupole resonance, for $\omega_{laser} \gg \omega_{res}$ or $\omega_{laser} \ll \omega_{res}$, the azimuthal dependence of the PAD disappears, and the images display the azimuthal symmetry expected for purely dipolar photoionization. Qualitatively similar results to the ones shown in Figs. 1 and 2 are obtained with the laser polarization in the plane of the imaging detector. In this case, a θ dependence of the PAD with respect to the laser polarization is observed that is common to photoionization experiments in the dipolar approximation, in addition to a symmetry breaking along the laser propagation direction that violates the dipolar approximation.

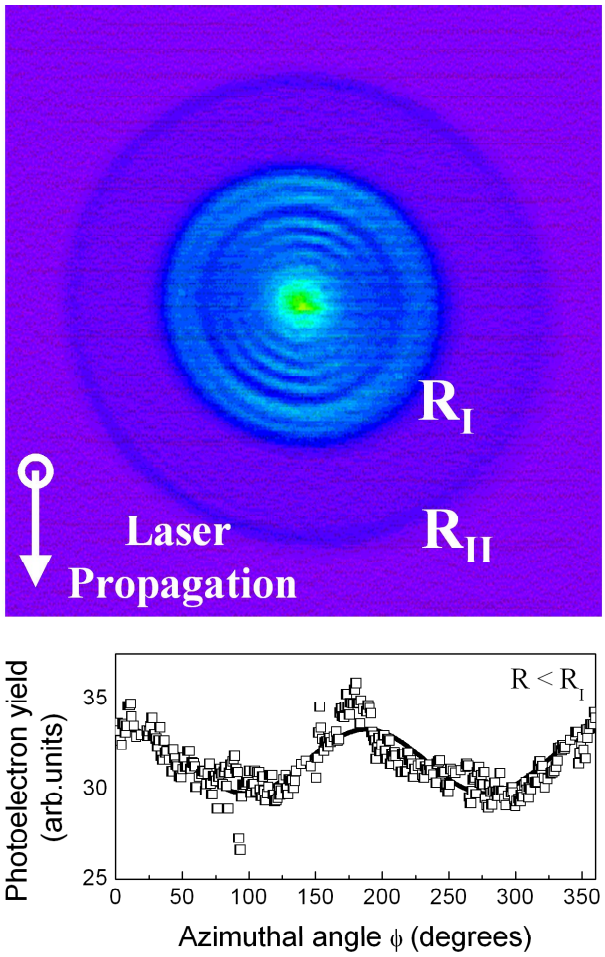

FIG. 1 (color online). (Upper panel) Two-dimensional photoelectron image recorded in (1 + 1) REMPI of metastable $Xe(6s[3/2]_2)$ using a tunable laser perpendicularly polarized to the detector plane and propagating from the top to the bottom of the image, with the laser tuned to the $6s[3/2]_{J=2} \rightarrow 5d[3/2]_{J=3}$ quadrupole-allowed resonance. (Lower panel) Experimental photoelectron angular distribution for the direct contribution (up to R_I, see text) derived from the image (squares) along with a fit (solid line) using Eq. (1). On resonance the quadrupolar selection rules introduce a $\cos^2\phi$ dependence in the azimuthal angular distribution.

The evolution of the asymmetry of the PADs as a function of wavelength, including the reversal of the asymmetry around the resonance, is further illustrated in Fig. 3. We define the asymmetry parameter κ that is plotted in Fig. 3 as the difference between the forward and the backward signal divided by the total signal. Far above or below the resonance, the asymmetry parameter is zero, as expected in the dipolar approximation. The asymmetry parameter is also zero on the resonance, but has a minimum and a maximum on either side of the resonance where the asymmetry is very large (i.e., more than 20% of the maximum possible value of ± 1 when all the signal is in the forward or the backward direction).

In order to understand this behavior of the PAD, a simple model based on a spherical harmonic expansion was used. The initial metastable Xe state is an s orbital ($l = 0$, $m_l = 0$). Following the dipolar selection rules for linearly polarized light, the nonresonant dipolar two-photon ionization channel (D/D) contributes two partial waves (0, 0) and (2, 0) to the PAD, whereas the (near)-resonant quadrupolar two-photon ionization channel (Q/D) contributes four partial waves (1, 1), (1, -1), (3, 1), and (3, -1). After some angular momentum algebra similar to the formalism developed by Dixit and Lambropoulos [15] one can the derive the following expression for the photoelectron angular distribution:

$$\frac{d\sigma}{d\phi} = \sigma_0[1 + C_{dq}|g(\omega)|^2(\omega_{\mathrm{res}} - \omega_{\mathrm{laser}})\cos(\varphi) + C_q|g(\omega)|^2\cos(\phi)^2], \quad (1)$$

where $g(\omega)$ is a line shape factor for the quadrupole resonance in the expression of the transition moment, ω_{laser} is the frequency of the laser and ω_{res} is the $6s[3/2]_{J=2} \rightarrow 5d[5/2]_{J=3}$ resonance frequency. The first (isotropic) term in the azimuthal angular distribution corresponds to a purely (nonresonant) dipolar two-photon ionization (D/D). The third term corresponds to resonant-enhanced two-photon ionization via the quadrupole resonance (Q/D). The second term is due to interference between the nonresonant (D/D) and the resonant (Q/D) channels.

According to this formula, the dipole approximation is valid far from the resonance ($\omega_{\mathrm{laser}} \gg \omega_{\mathrm{res}}$ or $\omega_{\mathrm{laser}} \ll \omega_{\mathrm{res}}$), when only the first term in Eq. (1) plays a role and the PAD does not depend on the azimuthal angle ϕ. On the resonance, the first and third terms are nonvanishing, and a sum of purely dipolar and quadrupolar terms is measured. The PAD now contains a $\cos^2(\phi)$ term, and electrons are symmetrically emitted in a direction that is preferentially forward or backward with respect to the propagation direction of the laser. Finally, close to the resonance, the second term becomes important and gives a forward/backward asymmetry, determined by the parameter C_{dq}.

A simple calculation shows that the asymmetry parameter k can be expressed as

$$\kappa = \frac{4C_{dq}}{\pi}|g(\omega)|^2\frac{\omega_{\mathrm{res}} - \omega_{\mathrm{laser}}}{C_q|g(\omega)|^2 + 2}. \quad (2)$$

C_q can be extracted from the image measured on resonance where the second term in Eq. (1) vanishes, while C_{dq} is obtained by fitting κ away from the resonance. A fit obtained with $C_q = 12 \pm 1$ and $C_{dq} = 1.31 \pm 0.05$ is shown in Fig. 3, and shows good agreement with the experiment.

The observation of a forward/backward asymmetry close to the resonance provides further insight into the occurrence of direct and indirect ionization events between the saddle point in the Coulomb + dc field potential and the field-free ionization limit. As observed in Figs. 2(a), 2(b), and 3(b), the asymmetry in the ring corresponding to direct ionization (extending up to R_{I}) is opposite from the asymmetry in the ring corresponding to indirect ionization (extending up to R_{II}). The direct contribution is due to electrons that travel along near-parabolic trajectories, where the azimuthal angle remains unchanged as the electron travels to the detector. As illustrated in Fig. 3(a), the indirect contribution corresponds to electrons with complex trajectories, where the

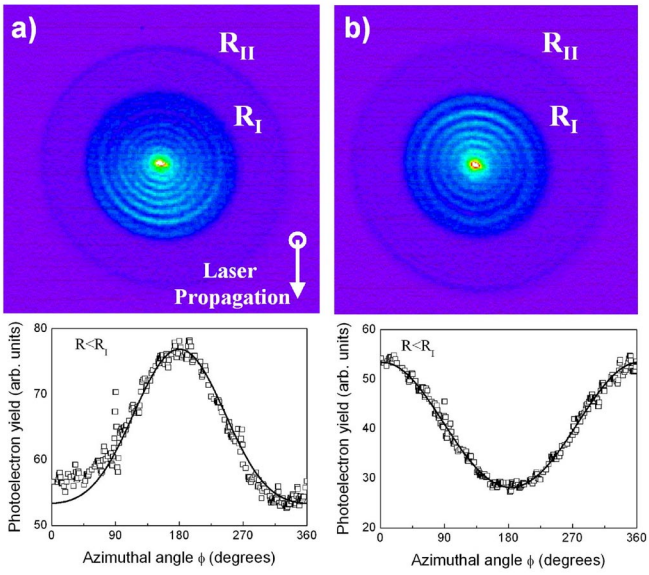

FIG. 2 (color online). Two-dimensional photoelectron images and photoelectron angular distributions recorded in (1 + 1) REMPI of metastable Xe($6s[3/2]_2$) using a tunable laser perpendicularly polarized to the detector plane and propagating from the top to the bottom of the images. The images were recorded at detunings of (a) -2.67 cm^{-1} and (b) $+2.05$ cm^{-1} from the $6s[3/2]_{J=2} \rightarrow 5d[3/2]_{J=3}$ quadrupole-allowed resonance. A forward/backward asymmetry along the laser propagation direction is observed, which is due to interference between dipole-allowed and quadrupole-allowed ionization channels. The lower plots show experimental photoelectron angular distributions (squares) along with a fit (solid line) according to Eq. (1), in both cases for the direct contribution (within $R < R_{\mathrm{I}}$, see text).

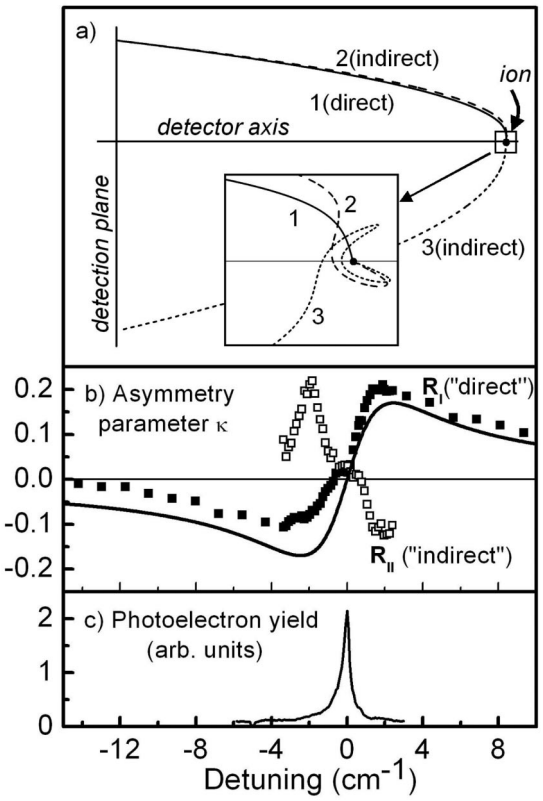

FIG. 3. (a) Sample trajectories for (1 + 1) REMPI of metastable Xe($6s[3/2]_2$) in an 825 V/cm electric field in the vicinity of the $6s[3/2]_{J=2} \rightarrow 5d[3/2]_{J=3}$ quadrupole resonance. Trajectory 1 is a direct trajectory where the electron does not cross the detector axis. Trajectories 2 and 3 are indirect trajectories that cross the detector axis once, respectively, twice on the way to the detector. (b) Measured asymmetry parameter $\kappa = (I_{\text{forward}} - I_{\text{backward}})/(I_{\text{forward}} + I_{\text{backward}})$ for the direct (solid squares) and indirect (open squares) ionization channels, as a function of the detuning from the $6s[3/2]_{J=2} \rightarrow 5d[3/2]_{J=3}$ quadrupole resonance, along with a fit of the asymmetry parameter for the direct channel according to Eq. (2). Both ionization channels show a forward/backward asymmetry that changes sign around the resonance. The asymmetry in the indirect ionization channel has the opposite sign from the asymmetry in the direct channel. (c) (1 + 1) REMPI efficiency around the $6s[3/2]_{J=2} \rightarrow 5d[3/2]_{J=3}$ quadrupole resonance.

electron may interact with the Xe^+ core (and cross the detector axis) one or more times. If the electron crosses the detector axis an odd number of times, then an electron emitted at an azimuthal angle ϕ is observed at detector angle $\phi + \pi$ so the azimuthal asymmetry is reversed. Indeed, Fig. 3(b) shows that near the resonance the asymmetry parameter for the indirect contribution has the opposite sign of the one for the direct channel. For a large negative detuning from the resonance (-4 cm^{-1}), the direct contribution remains strongly asymmetric, whereas the asymmetry parameter for the indirect contribution goes to zero. Close to the resonance, the indirect contribution is dominated by trajectories where the electron crosses the symmetry axis of the detector just once, whereas farther away from the resonance the indirect contribution contains roughly equal amounts of trajectories that cross the detector axis once, respectively, twice.

In conclusion, we have observed a very strong azimuthal dependence of the PAD in a two-photon ionization experiment with excitation on or near a quadrupole resonance, with a forward/backward asymmetry in the PAD that can be as large as 20%. The trends in the PAD are well reproduced by a simple model, where the asymmetry arises as a consequence of interference between two ionization channels. Finally, when threshold photoelectrons are produced in the ionization, the observed asymmetries provide insight into the nature of the classical electron trajectories.

This work is part of the research program of FOM (Fundamental Research on Matter), which is subsidized by the NWO (Netherlands Organization for the Advancement of Research). Further support from the Van Gogh Program, the EU Marie Curie Individual Fellowship Program (S. Z.), and the EU research training network HPRN-2002-00183 (PICNIC) is gratefully acknowledged.

*Permanent address: Laboratoire de Spectrométrie Ionique et Moléculaire, UMR CNRS 5579, Bâtiment A. Kastler, 43 Boulevard du 11 Novembre 1918, 69622 Villeurbanne cedex, France.

[1] B. Krässig *et al.*, Phys. Rev. Lett. **88**, 203002 (2002).
[2] O. Hemmers *et al.*, Phys. Rev. Lett. **91**, 053002 (2003).
[3] E. P. Kanter *et al.*, Phys. Rev. A **68**, 012714 (2003).
[4] O. Hemmers, R. Guillemin, and D.W. Lindle, Radiat. Phys. Chem. **70**, 123 (2004).
[5] G. Leuchs, S. J. Smith, S. N. Dixit, and P. Lambropoulos, Phys. Rev. Lett. **56**, 708 (1986).
[6] P. Lambropoulos, G. Doolen, and S. P. Rountree, Phys. Rev. Lett. **34**, 636 (1975).
[7] M. Lambropoulos, S. E. Moody, S. J. Smith, and W. C. Lineberger, Phys. Rev. Lett. **35**, 159 (1975).
[8] A. Dodhy, R. N. Compton, and J. A. D. Stockdale, Phys. Rev. A **33**, 2167 (1986).
[9] A. Lyras *et al.*, Phys. Rev. A **37**, 403 (1988).
[10] A. T. J. B. Eppink and D. H. Parker, Rev. Sci. Instrum. **68**, 3477 (1997).
[11] H. L. Offerhaus, C. Nicole, F. Lépine, Ch. Bordas, F. Rosca-Pruna, and M. J. J. Vrakking, Rev. Sci. Instrum. **72**, 3245 (2001).
[12] Ch. Bordas, Phys. Rev. A **58**, 400 (1998).
[13] C. Nicole, I. Sluimer, F. Rosca-Pruna, M. Warntjes, M. Vrakking, Ch. Bordas, F. Texier, and F. Robicheaux, Phys. Rev. Lett. **85**, 4024 (2000).
[14] C. Nicole, H. L. Offerhaus, M. J. J. Vrakking, F. Lépine, and Ch. Bordas, Phys. Rev. Lett. **88**, 133001 (2002).
[15] S. N. Dixit and P. Lambropoulos, Phys. Rev. A **27**, 861 (1983).